

Magnetic circular dichroism and Faraday rotation spectra of $Y_3Fe_5O_{12}$

G. B. Scott, D. E. Lacklison, H. I. Ralph, and J. L. Page

Mullard Research Laboratories, Redhill, Surrey, England

(Received 17 March 1975)

The magnetic circular dichroism (MCD), Faraday rotation (FR), and absorption spectra of $Y_3Fe_5O_{12}$ at 77 K are presented between 10000 and 25000 cm^{-1} . Comparison of MCD and FR line shapes with absorption-band energies indicates that the Fe^{3+} crystal-field transitions are predominantly paramagnetic in nature. It is shown that spin-orbit mixing of the ${}^4T_{1g}(G)$ excited crystal-field states into the ground state is sufficient to explain the observed MCD of the ${}^6A_{1g}(S) \rightarrow {}^4T_{1g}(G)$ band without producing an unacceptable change in the ground-state g factor and is consistent with the observation of paramagnetic line shapes for the other Fe^{3+} crystal-field transitions. It is pointed out that previous analyses of the magneto-optical spectra of iron garnets above 20000 cm^{-1} are probably in error.

I. INTRODUCTION

Since the early Faraday-rotation (FR) measurements on $Y_3Fe_5O_{12}$ (YIG) by Dillon,¹ there has been much work on the various aspects of FR in rare-earth iron garnets, e.g., wavelength dependence in the infrared,^{2,3} effects of rare-earth ions,^{4,5} temperature dependence,^{4,6} effects of ions with large spin-orbit interactions,^{7,8} *inter alia*. However, there has, until recently, been little work directed towards obtaining a comprehensive FR spectrum of YIG. Dillon⁹ has presented the FR spectrum at 1.5 K to 20 500 cm^{-1} using thin crystal sections but with little analysis. Kuse *et al.*¹⁰ reported the FR spectrum from 5000 to 20 000 cm^{-1} on single crystals of YIG at 81 and 295 K, and most recently a series of measurements on epitaxially grown YIG have been published¹¹⁻¹³ which, owing to the thinness of the layers, tend to concentrate on the FR spectrum above 16 000 cm^{-1} . With a few exceptions, the structure in the FR spectrum of YIG is not clearly correlated with observed optical transitions; this arises from the overlapping contributions of the many transitions and the dispersive nature of the Faraday rotation. For this reason we have measured both magnetic circular dichroism (MCD) and FR spectra to aid the analysis.

MCD spectra are in general simpler to interpret than FR spectra owing to the localized nature of the absorption. Until recently, MCD spectra were not directly available for YIG although similar data had been obtained^{13,14} from Kerr ellipticity and rotation experiments for energies above 20 000 cm^{-1} . Canit *et al.*¹⁵ have reported MCD data on YIG in the range 13 000 to 32 000 cm^{-1} and their results are in agreement with MCD data presented here. Again the interpretation of the MCD spectrum is not straightforward, owing to the overlapping of many components, and we have found it necessary to use MCD, FR, and absorption spectra to aid the analysis.

II. EXPERIMENTAL

Absorption data were taken using Hitachi EPS and Cary 17R spectrophotometers; data were reflection corrected. Faraday rotation was measured using a polarization-modulation technique allowing rotations to be obtained to better than 0.01° ; samples were saturated in a solenoid producing 0.3 T. MCD spectra were obtained using a quartz piezobirefringent modulator. Corrections for Dewar windows were necessary only for FR data.

All measurements were performed on slices of YIG cut from bulk crystals grown from PbO - PbF_2 fluxes (Pb content of < 300 ppm). Samples produced by Syton polishing such slices had thicknesses down to 2 μm ; ion-beam thinning was used to produce 0.5- μm -thick sections. Sample thicknesses, determined by interferometry for the thinnest samples (< 10 μm) and an electromechanical instrument for thicker samples, were the largest sources of error in determining absolute FR, MCD, and absorption coefficient. This error is not expected to exceed 5%, being largest for the thinnest samples. The highest-energy MCD data were taken on a YIG film which was rf sputtered onto a $Gd_3Ga_5O_{12}$ substrate and subsequently annealed in oxygen. We have found that such films exhibit very similar optical properties to bulk-grown YIG.¹⁶ It is worth noting that YIG films grown by liquid-phase epitaxy from lead-based fluxes can contain substantial levels of Pb^{2+} (Ref. 17), whose presence has been detected optically¹⁸ through observation of the ${}^1S_0 \rightarrow {}^3P_1$ transition of this ion at 36 000 cm^{-1} . The Fe^{4+} ion may be induced to charge compensate for Pb^{2+} and if octahedrally coordinated the ${}^5T_{2g} \rightarrow {}^5E_g$ transition is to be expected around 20 000 cm^{-1} . It is also known that Pb^{2+} in YIG greatly affects the magneto-optical properties⁹ and care should be exercised when comparing bulk-grown single-crystal data with epitaxial-film data.

III. MAGNETO-OPTIC RELATIONSHIPS

Phenomenologically, magneto-optic effects in dielectrics can be described by the dielectric tensor

$$\epsilon = \begin{pmatrix} \epsilon_0 & -i\epsilon_1 & 0 \\ i\epsilon_1 & \epsilon_0 & 0 \\ 0 & 0 & \epsilon_z \end{pmatrix},$$

where we have assumed for simplicity that the material is nonpleochroic and that the magnetization is parallel to the positive z direction in a right-handed set of axes.

The normal modes of propagation of light through this system consist of right and left circularly polarized (RCP and LCP) components traveling along the positive z direction. We use the definition that light is RCP if on looking against the direction of propagation, the electric vector rotates counterclockwise; we assume the field vector to propagate as $e^{-i\omega t}$. The complex refractive indices N_+ and N_- of RCP and LCP, respectively, are related to ϵ_0 and ϵ_1 by

$$N_{\pm}^2 = \epsilon_0 \pm \epsilon_1,$$

where

$$N_{\pm} = n_{\pm} + ik_{\pm}, \quad \epsilon_0 = \epsilon'_0 + i\epsilon''_0, \quad \epsilon_1 = \epsilon'_1 + i\epsilon''_1,$$

and n_{\pm} and k_{\pm} are the refractive indices and extinction coefficients of LCP and RCP.

It is simple to show that the Faraday rotation of a linearly polarized beam of vacuum wavelength λ_0 is

$$\theta = -(\pi/\lambda_0)(n_+ - n_-) \text{ rad/cm},$$

where we use the definition that FR is positive if, on traversing the sample along the direction of magnetization, the direction of linear polarization rotates counterclockwise when viewed against the direction of propagation.

The MCD is defined in terms of the extinction coefficients k_{\pm} as

$$\Delta\alpha = \alpha_+ - \alpha_- = (4\pi/\lambda_0)(k_+ - k_-) \text{ cm}^{-1}.$$

The components ϵ'_1 and ϵ''_1 are related to θ , $\Delta\alpha$, n , and k by

$$\begin{aligned} \epsilon'_1 &= -(\lambda_0/\pi)(n\theta + \frac{1}{4}k\Delta\alpha), \\ \epsilon''_1 &= -(\lambda_0/\pi)[\theta k - n(\frac{1}{4}\Delta\alpha)], \end{aligned}$$

where $n = \frac{1}{2}(n_+ + n_-)$ and $k = \frac{1}{2}(k_+ + k_-)$.

Traditionally, magneto-optic line shapes are classified as paramagnetic or diamagnetic having the forms shown in Fig. 1. In isolated magneto-optically active ions paramagnetic line shapes appear when the ion has a finite orbital angular momentum in its ground term, and diamagnetic line shapes appear when it has a finite orbital angular

momentum in the excited term. In a magnetically ordered system the exchange field and spin-orbit coupling act together to give a strong effective external field, which not only enhances the strength of these lines but also causes dipole-forbidden transitions to exhibit paramagnetic lines by making the oscillator strengths for right and left circularly polarized light different. This view of the origin of the two magneto-optic line shapes in magnetically ordered material has been held until recently, when several complications became apparent. A fuller discussion of the necessary changes to the theory is given in Sec. V.

Up to $20\,000 \text{ cm}^{-1}$, the values of n and k for¹⁴ YIG are such that the approximations

$$\epsilon'_1 = -(\lambda_0/\pi)n\theta,$$

$$\epsilon''_1 = \lambda_0 n \Delta\alpha / 4\pi,$$

are within 5% and 1%, respectively, of the results obtained using the full expressions. It is therefore quite acceptable to take the line-shape functions of θ and $\Delta\alpha$ as those of ϵ'_1 and ϵ''_1 , respectively (see Fig. 1). For the highest energy spectrum shown, the approximation is not as good as above but the qualitative relationships between the line shapes should still be reasonably well obeyed.

In the above we have neglected the effects of the boundaries of the sample on the measured FR and MCD. As will be seen, these effects become important in the regime where the complex rotation experienced on transmission through the sample is of the same order as that experienced on reflection, i. e., for the thin samples which are necessary to measure the spectra of materials in

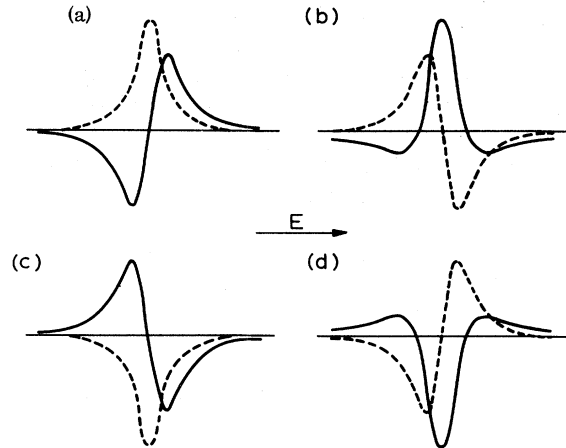


FIG. 1. Line shapes of off-diagonal dielectric-tensor elements $\epsilon_1 = \epsilon'_1 + i\epsilon''_1$: (a) Positive paramagnetic line shapes; (b) positive diamagnetic line shapes; (c) negative paramagnetic line shapes; (d) negative diamagnetic line shapes. ϵ'_1 , —; ϵ''_1 , ---; see text for relationship between ϵ'_1 , ϵ''_1 and FR and MCD.

TABLE I. Position of magneto-optic features listed versus line shape and assignment.

Energy (cm ⁻¹)	Line shape		Band assignment
	Paramagnetic	Diamagnetic	
10 400	+		⁶ A _{1g} (⁶ S) → ⁴ T _{1g} (⁴ G)
10 920	+		
11 420	+		
13 500	+		⁶ A _{1g} (⁶ S) → ⁴ T _{2g} (⁴ G)
14 090	-		
14 870	-		
16 050	+		⁶ A ₁ (⁶ S) → ⁴ T ₁ (⁴ G)
16 500	+		
16 840	-		
17 380	+		
18 200	+		biexciton or Fe ³⁺ -Fe ³⁺ charge transfer
18 550	+		
19 100	-		
19 600	+		
20 700	+		
21 500	+		
22 500	+		
23 250		+	
25 200	-		
27 500	-		

the regions of high absorption.

It can be shown that the complex rotation Φ suffered by a linearly polarized beam after transmission through a free-standing sample of thickness L is

$$\Phi = \left(-\frac{\pi L}{\lambda_0} + \frac{i(N_+ - 1)}{2N(N_+ + 1)} \right) (N_+ - N_-),$$

where $N = \frac{1}{2}(N_+ + N_-)$.

The first term in large parentheses describes the effects due to passage through the bulk of the material and the second, the effects of the two interfaces. Using known values of θ , $\Delta\alpha$, n , and k for¹⁴ YIG in the above expression we have estimated that for a 0.5- μ m-thick sample, the boundary contribution to the rotation of the plane of polarization is only of order 2% of that caused by passage through the bulk. We are therefore justified in neglecting boundary effects in our data.

IV. SPECTRA

In this section we shall present and interpret the spectra for which a summary of the relevant details is given in Table I. Figure 2 shows the MCD, FR, and absorption spectrum of the ⁶A_{1g}(⁶S) → ⁴T_{1g}(⁴G) band at 77 K. The three major components in absorption at 10 400, 10 920, and 11 420 cm⁻¹ are shown to be associated with positive paramagnetic terms in the MCD (Fig. 1), the two former being particularly strong. The weak, sharp absorption band at 10 140 cm⁻¹ appears to be associated with the shoulder on the low-energy

side of the MCD peak at 10 400 cm⁻¹. The FR spectrum corresponding to the above major MCD features should consist of three dispersive-shaped lines, negative going at energies below the transition resonance energy, positive going above (we shall refer to them as positive dispersive line shapes, see Fig. 1). The presence of a strongly rising FR background arising from higher-energy transitions tends to obscure this behavior; compression of the energy scale allows detection of these features more readily. We are unable to make an assessment of the line shape of the MCD arising from the 10 140-cm⁻¹ absorption band due to lack of experimental resolution and the proximity of the 10 400-cm⁻¹ band; the FR spectrum does not offer any help in this region.

Comparison of the absorption spectrum with the MCD and FR spectra for transitions between 12 000 and 20 000 cm⁻¹, shown in Fig. 3, reveals that the magneto-optic spectra have resolved more components than straight absorption. Owing to the rather featureless nature of the absorption bands, interpretation of the MCD line shapes and their correlation with the absorption spectrum is not straightforward. However, the combination of FR and MCD allows us to make fairly definite line-shape determinations.

The ⁶A_{1g}(⁶S) → ⁴T_{2g}(⁴G) band is resolved into three MCD paramagnetic terms centered at 13 500, 14 090, and 14 870 cm⁻¹ (Fig. 3), only the first of which is positive. The negative MCD peak at 14 870

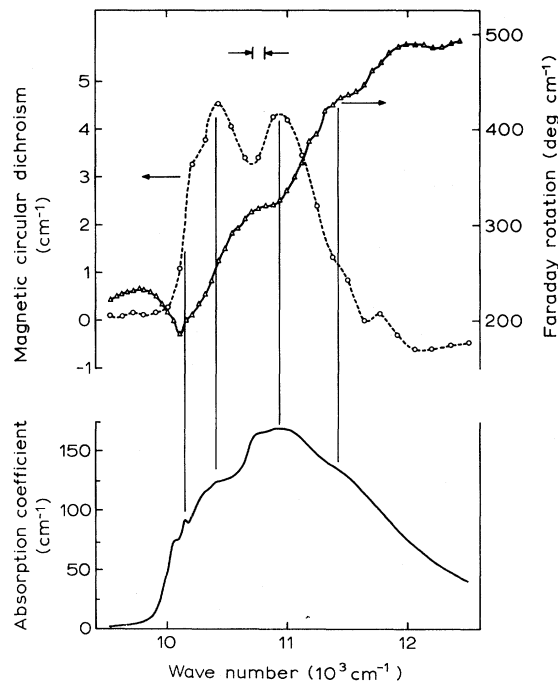


FIG. 2. MCD, FR, and absorption spectra in the region of the ⁶A_{1g}(⁶S) → ⁴T_{1g}(⁴G) band in YIG at 77 K.

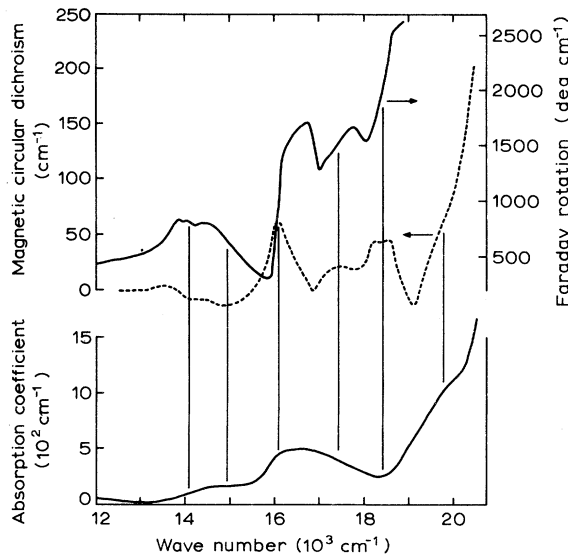


FIG. 3. MCD, FR, and absorption spectra of YIG between 12 000 and 20 000 cm^{-1} at 77 K.

cm^{-1} is associated with a clear negative FR dispersive line shape, whereas the FR line shapes of the lower-energy components are not well resolved. It is worth noting that the MCD of the ${}^6A_{1g}(S) \rightarrow {}^4T_{2g}(G)$ band is predominantly negative while that of the ${}^6A_{1g}(S) \rightarrow {}^4T_{1g}(G)$ band is positive, a feature shared by the isoelectronic ion Mn^{2+} in both tetrahedral¹⁹ and octahedral²⁰ coordination. This fact indicates that it is unwise to make assignments of bands to either the octahedral or tetrahedral sublattice on the basis of the sign of the MCD or FR as has been done previously by other authors.

The MCD of the ${}^6A_{1g}(S) \rightarrow {}^4T_{1g}(G)$ band consists of three positive paramagnetic components at 16 050, 17 380, and approximately 16 500 cm^{-1} , the latter being a weaker component on the edge of the 16 050- cm^{-1} band (Fig. 3). The FR spectrum supports the assignments of these line shapes for the two well-resolved MCD peaks. The 77-K absorption spectrum of this band is rather featureless but the components resolved at 4.2 K¹⁶ agree well in energy with the above centers of MCD. There seems to be some indication of a negative paramagnetic component at 16 840 cm^{-1} , the center of which coincides with the center of the corresponding feature in the FR. In fact, at 6 K this feature is even more distinct and gives rise to a peak which lies below the MCD baseline.¹⁵ This feature has not been seen in absorption at 4.2 K.

The remaining features in the MCD before the onset of the strong edge at 20 000 cm^{-1} appear to consist of two positive paramagnetic components at 18 200 and 18 550 cm^{-1} , a negative peak at 19 100 cm^{-1} , and a shoulder with a center around 19 600 cm^{-1} . The two overlapping positive paramagnetic

MCD bands at 18 200 and 18 550 cm^{-1} are well correlated with a positive FR dispersive line shape. No structure in the absorption spectrum has been resolved corresponding to these magneto-optic features and it is not clear whether they are associated with the high-energy tail of the ${}^6A_{1g}(S) \rightarrow {}^4T_{1g}(G)$ band or the low-energy side of the ${}^6A_{1g}(S) \rightarrow {}^4T_{2g}(G)$ transition. The features at 19 100 and 19 600 cm^{-1} coincide with components resolved at 4.2 K in direct absorption.¹⁵

Although the feature of the MCD spectrum reported in this region agree with those of Canit *et al.*,¹⁵ their data in the region of 20 000 cm^{-1} appear to be superimposed on a broad positive background; e.g., the negative MCD peak in our data at 19 100 cm^{-1} (Fig. 3) is shown in the data of Ref. 14 to be a local minimum on a positive background. We believe this background is due to the incorporation of Pb^{2+} in the epitaxial YIG film used by Canit *et al.* Lead is known to be incorporated in epitaxially grown YIG more easily than into bulk-grown crystals.¹⁷ Full verification of this point awaits MCD measurements on crystals deliberately doped with Pb^{2+} , but we have made measurements on YIG doped with Bi^{3+} , whose magneto-optic effect on YIG is similar to that of Pb^{2+} with which it is isoelectronic.⁸ The MCD of YIG:Bi is shown in Fig. 4. Compared to the MCD of YIG free from lead and bismuth the increases shown in Fig. 4 due

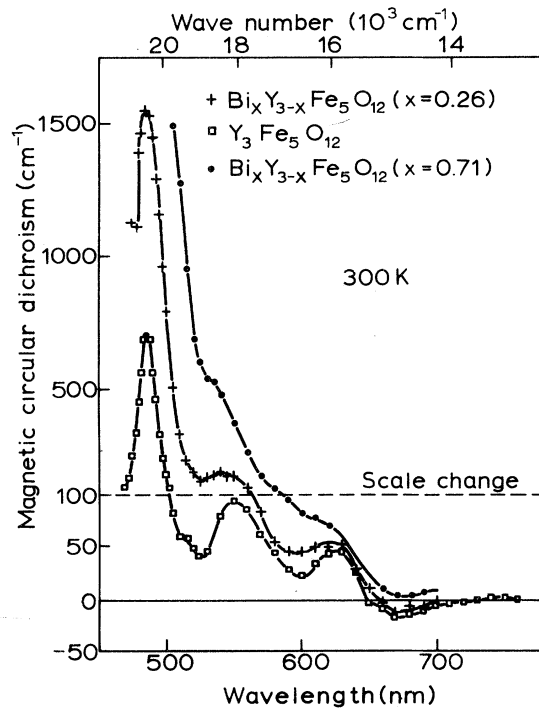


FIG. 4. Effects of Bi^{3+} on the MCD spectrum of YIG between 12 000 and 21 000 cm^{-1} at 300 K.

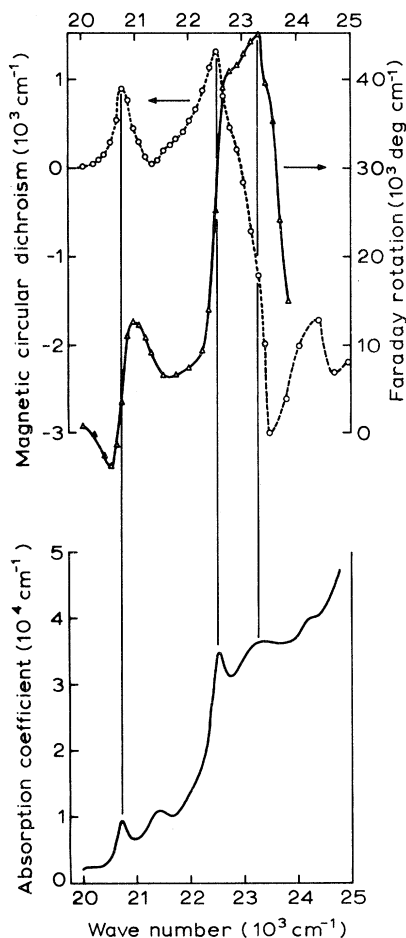


FIG. 5. MCD, FR, and absorption spectra of YIG between 20 000 and 25 000 cm^{-1} at 77 K.

to Bi^{3+} are larger than those shown by Canit *et al.*¹⁵ and presumed to be due to Pb^{2+} . This is consistent with lower expected lead concentrations relative to the bismuth concentrations and with the smaller effectiveness of Pb^{2+} compared to Bi^{3+} .

Figure 5 shows a particularly well-resolved positive paramagnetic MCD peak centered at 20 700 cm^{-1} and coinciding with the ${}^6A_1(S) \rightarrow {}^4E; {}^4A_1(G)$ band the FR shows a clearly defined positive dispersive line shape. The onset of a positive shoulder at 21 500 cm^{-1} in the MCD presumably arises from the ${}^6A_{1g}(S) \rightarrow {}^4E_g; {}^4A_{1g}(G)$ transition at 21 400 cm^{-1} and an unassigned transition at 21 640 cm^{-1} (Ref. 16). Centered at 22 500 cm^{-1} is yet another positive dispersive line shape in the FR spectrum whose center is that of a corresponding, strong MCD peak and absorption band, the ${}^6A_{1g}(S) \rightarrow {}^4T_{2g}(D)$ transition.¹⁶ It is around this energy that the character of the MCD spectrum changes. To 22 500 cm^{-1} the MCD spectrum consists predominantly of positive paramagnetic contributions, while between 22 500 and 28 500 cm^{-1} this is re-

versed, as can be seen in Figs. 5 and 6. The coincidence of a strong positive peak in the FR spectra, a strong negative dispersive line shape in the MCD, and a strong component in the absorption spectrum centered at 23 250 cm^{-1} (Fig. 5) indicates the appearance of a diamagnetic magneto-optic component. This transition is of particular interest for its involvement in the large Bi^{3+} -induced FR in iron garnets^{7,21} and for its concentration dependence.¹⁶ At 23 250 cm^{-1} , where the center of the negative dispersive line shape lies, the MCD has a value of approximately -1500 cm^{-1} (Fig. 5), suggesting that it is superimposed on another component.

The appearance of two negative MCD peaks at 25 200 and 27 500 cm^{-1} corresponds to strong components in the absorption spectrum at these energies in YIG.¹⁶

V. DISCUSSION

The most striking feature of the magneto-optic spectrum of YIG to 29 000 cm^{-1} is the predominance of paramagnetic transitions; indeed only one appears to be diamagnetic. We will show in a later paper that this situation pertains to even higher energies.

A qualitative theory of the magneto-optic properties of crystals containing concentrated transition-metal ions with particular reference to the oxides of Fe^{3+} has been discussed extensively in the literature.^{4,14,22} It has now long been known that if a magneto-optically active paramagnetic center has no orbital degeneracy in its ground state it will always exhibit only a diamagnetic effect. This is seen for example with $6s^2$ ions such as Tl^+ and Pb^{2+} and with color centers such as F centers²⁴ and U_2 centers²⁵ in alkali halides.

Except in special cases the same diamagnetic line shape is predicted for transition-metal ions with S ground terms in an exchange field by a theory due to Crossley *et al.*⁴ On the other hand a

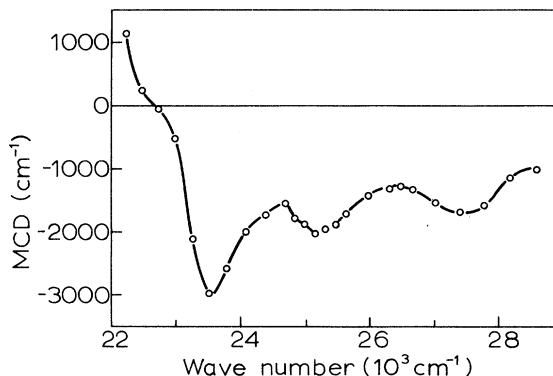


FIG. 6. MCD spectrum of an rf-sputtered YIG film at 77 K between 22 000 and 28 000 cm^{-1} .

paramagnetic FR is observed in YIG for the crystal-field transitions of Fe^{3+} whose ground term is an orbital singlet. An explanation for this line shape was given by Clogston,²² who studied in detail the forbidden ${}^6A_{1g}(S) \rightarrow {}^4T_{1g}(G)$ transition and showed that the optical transition could be made allowed by mixing these two terms into each other with the spin-orbit interaction and mixing a 6P charge-promoted or charge-transferred excited term into the ground 6S term with odd-parity phonon displacements. He then showed that exactly the same mixing gave rise to a paramagnetic line in the FR. This position was formalized by Kahn *et al.*,¹⁴ who suggested that for the Fe^{3+} -oxide crystals the allowed charge-transfer transitions would show diamagnetic magneto-optic effects and the forbidden crystal-field transitions would show paramagnetic effects. Kahn *et al.* were able to interpret their extensive data from ferric oxides in these terms. This interpretation has become generally accepted as correct^{12-14,26} and attempts have been made to use the magneto-optic line shapes to identify the allowed and forbidden transitions in the region 20 000–35 000 cm^{-1} in YIG and related iron garnets.

Quite recently this useful picture has been upset by Cheng's observation²⁷ of a paramagnetic magneto-optic line shape associated with the allowed charge-transfer transitions of Fe^{3+} in MgO . Cheng's observation is consistent with the theory of Crossley *et al.*,⁴ which indicates that there should be no distinction between allowed and forbidden transitions. They show that if the spin-orbit mixing between different terms is neglected the magneto-optic line shape associated with transitions involving ions with orbital singlet ground states is diamagnetic. This conclusion does not depend on the transitions being allowed or forbidden. They show also that when the spin-orbit mixing between different terms is included a paramagnetic line is predicted. For example, the spin-orbit mixing of the excited 4T_2 term of Cr^{3+} into the 4A_2 ground term is sufficiently strong to give observable paramagnetic lines.²⁸ This same splitting gives a deviation Δg of the spectroscopic splitting factor from the electron-spin value of 2, and the strength of the paramagnetic line becomes proportional to Δg . We show later that a similar mixing can be expected in Fe^{3+} and is of sufficient magnitude to account for the observed paramagnetic magneto-optic effect but gives very little change of g from the value of 2.

The theory given by Clogston²² for Fe^{3+} is probably qualitatively correct for ions isolated in diamagnetic lattices but we now show that the data presented here and the structure found in the low-energy tail of the ${}^6A_{1g}(S) \rightarrow {}^4T_{1g}(G)$ band taken by van der Ziel *et al.*²⁹ make it unlikely to be the

mechanism operating in YIG. Using Clogston's expressions (8) and (9) gives for the dichroism

$$\Delta\alpha/\alpha = (1 + \delta)^2 - (1 - \delta)^2,$$

where

$$\delta = \frac{u}{\Delta} \frac{W}{\Delta - W}.$$

Here W is the separation of the ${}^6A_{1g}(S)$ and the ${}^4T_{1g}(G)$ terms on the octahedral site, Δ is the separation between the ground and the charge-transferred excited terms, and u is the splitting of the orbital part of the charge-transferred term in the exchange field. Since the exchange field can affect the orbital motion only through the spin-orbit interaction the value of u is not likely to be larger than the 100 cm^{-1} suggested by Clogston. Clogston assumed that $\Delta \approx 2 \times 10^4 \text{ cm}^{-1}$, but it is now known^{16,30} that the relatively strong absorption between about 24 000 and 35 000 cm^{-1} is not due to charge-transfer transitions as was previously assumed.^{13,14,22} Putting $W = 10^4 \text{ cm}^{-1}$, $\Delta = 4 \times 10^4 \text{ cm}^{-1}$, and $u = 100 \text{ cm}^{-1}$ gives 0.3% for the MCD, much less than the 3% observed for this transition.

van der Ziel *et al.*²⁹ have studied the detailed structure of the low-energy tail of the ${}^6A_{1g}(S) \rightarrow {}^4T_{1g}(G)$ transition and observed two sharp magnetic dipole lines at 9783.5 and 9803.8 cm^{-1} , just below the onset of the main absorption band. These were assigned to pure electronic transitions. Their data, reproduced in Fig. 7, also shows electric dipole peaks at 10 073.1, 10 093.1, 10 126.7 and 10 146.8 cm^{-1} . The positions of these peaks relative to the magnetic dipole lines correspond to the positions of peaks in an empirically derived one-magnon density of states and they were tentatively assigned to magnon sidebands. It can be seen from Fig. 7 that the two main peaks in this region are reflected at energies higher by approximately 274

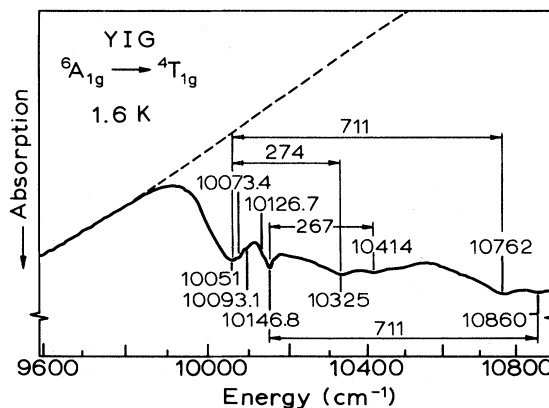


FIG. 7. Absorption spectrum of ${}^6A_{1g}({}^6S) \rightarrow {}^4T_{1g}({}^4G)$ band in YIG (Ref. 25) showing phonon sidebands of exciton-magnon (magnon sideband) lines.

and 711 cm^{-1} . These two separations agree with the energies of two Raman-active phonons found by Song *et al.*³¹ This suggests that in this region the absorption is due to phonon sidebands of the one-magnon sidebands. The even parity of these phonons contrasts with the odd parity required by the mechanism of Clogston.

The underestimate of the MCD and the difficulty with the phonon parity together make it unlikely that the mechanism of Clogston is responsible for the magneto-optic activity in this region of the spectrum.

We now propose a mechanism alternative to that of Clogston which we show can give an MCD of the observed magnitude. The oscillator strengths of the absorption bands of YIG: YGdG (yttrium gadolinium garnet) alloys below $20\,000 \text{ cm}^{-1}$ have been known for a long time to be strongly dependent on iron concentration.^{16,32,33} It is normally assumed that this sort of behavior is caused by the exchange-induced dipole mechanism³⁴ present when the ions exist in clusters of two or more.

There are two possible ways in which the inter-term mixing can give rise to a paramagnetic magneto-optic line shape. First, it can mix an excited term with an orbital degeneracy into the ground term, thereby imparting an orbital character to the ground term. Second, it can mix the states of different terms together by different amounts depending on whether the orbital parts are polarized parallel or antiparallel to the spin. These two mixings can be expected to be equally effective. An example of the second type was discussed in some detail by Cheng²⁷ and we now give a brief discussion of the first.

The only states which have finite matrix elements of the spin-orbit interaction with the 6A_1 ground term of Fe^{3+} are the $J = \frac{5}{2}$ levels of the three 4T_1 terms.³⁵ These matrix elements are tabulated by Schroeder,³⁶ but such tables are apparently subject to error³⁷ and we have checked the results we require. Figure 8 shows the strength β of the admixture of the three different ${}^4T_1 J = \frac{5}{2}$ levels into the ground state against the crystal-field parameter, using values for B and C of 700 and 2600 cm^{-1} , respectively, and a spin-orbit coupling constant of 350 cm^{-1} . The crystal-field parameter for YIG for Fe^{3+} at the octahedral site is around $13\,000 \text{ cm}^{-1}$ and consequently we see that the amount of 4T_1 -term mixed into the ground state is around 5%. This is sufficient to explain the magnitude of the observed fractional dichroism $(\alpha_+ - \alpha_-)/\alpha$ for the ${}^6A_{1g}(S) - {}^4T_{1g}(G)$ band assuming that the exchange-induced dipole operator joins the 6A_1 part and the 4T_1 part of the ground term to the excited term equally well.

Contrary to the case of Cr^{3+} (Ref. 4), the admixture of the 4T_1 levels into the 6A_1 levels has

only a second-order effect on the g value because the operator $\bar{L} + 2\bar{S}$ has no matrix elements between 4T_1 and 6A_1 terms. The magnitude of $\Delta g = g - 2$ then depends only on the square of the mixing coefficients. If the states of the ground term are given by

$$|a\rangle = \frac{1}{N} \left(|{}^6A_1\rangle + \sum_{\alpha} \beta_{\alpha} |{}^4T_1\rangle \right),$$

where N is a normalizing constant and α runs over the three 4T_1 terms of d^5 , the change of g is given by

$$\Delta g = \sum_{\alpha} \beta_{\alpha}^2 (g_{\alpha} - 2),$$

where g_{α} are the g values of the 4T_1 terms. Δg is also plotted in Fig. 8, where it can be seen that the contribution to Δg from this source is very small ($\sim 10^{-3}$), as is observed experimentally for Fe^{3+} in diamagnetic garnet hosts.³⁸ This change in the g factor, unlike the Cr^{3+} situation, is not proportional to the strength of the paramagnetic term in the magneto-optic effect.

These two mechanisms are capable of accounting qualitatively for the observed magnitude of all the paramagnetic lines in the magneto-optic spectrum which are associated with crystal-field transitions. More detailed explanations of the origins of the several components of each band would require much more theoretical effort. A study of the optical and magneto-optical properties of Fe^{3+} in much simpler systems than garnets will be of considerable help in advancing the understanding of iron garnet spectra.

It is more difficult to account for the magneto-optic spectrum corresponding to the region between $24\,000$ and $36\,000 \text{ cm}^{-1}$ of intermediate absorption. Now that it is understood that this is not the $\text{O}^{2-} - \text{Fe}^{3+}$ charge-transfer region^{16,30,33} it would seem most likely that the absorption is due to a combination of biexciton excitations, that is, crystal-

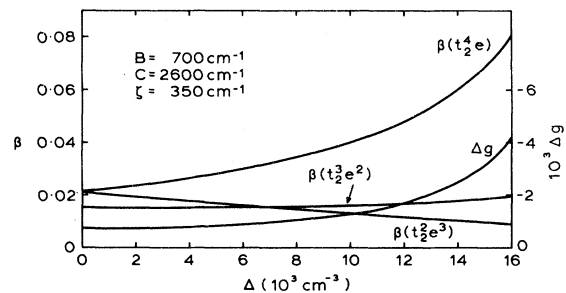


FIG. 8. Strength β of the admixture of the three $J = \frac{5}{2}$, 4T_1 levels into the ground state as a function of crystal-field strength. Also plotted versus crystal-field strength is the change Δg in the ground-state g factor as a result of the mixing.

field transitions on two neighboring ions simultaneously,¹⁶ and charge-transfer excitations where the charge is transferred between two Fe^{3+} ions making an $\text{Fe}^{4+}:\text{Fe}^{2+}$ pair.²⁶ The strength of the absorption due to either of these mechanisms will be decreased by dilution of the magnetic ions on either of the two sublattices. The biexciton excitations are understood in terms of the exchange-induced dipole mechanisms and they are well known in pairs of several transition-metal ions.³⁹ The positions of the peaks in the absorption spectrum of YIG can be correlated with the expected positions of the biexciton peaks.¹⁶

The possibility of spectra corresponding to charge transfer between metal ions was proposed long ago to account for bands associated with metal-ion clusters.⁴⁰ It should be treated with caution, however, when Fe^{3+} ions are involved because there is little definite evidence that Fe^{4+} can exist in any crystal. The strongest evidence is in recent optical-absorption data of Faughnan⁴¹ from iron-doped titanium oxides, which strongly suggests Fe^{4+} ions being present.

In YIG the most prominent iron-iron charge-transfer transition would be between octahedral and tetrahedral pairs. From consideration of the relative sizes of Fe^{2+} and Fe^{4+} ions and the relative sizes of the iron sites, the lowest-energy transition would be expected to transfer an electron from the tetrahedral to the octahedral site. This view is also supported by the observation that the O^{2-} -to- Fe^{3+} charge-transfer transition occurs at higher energies for tetrahedrally coordinated iron than for octahedrally coordinated iron.⁴²

Because the dipole operator is a one-particle operator, the allowed iron-iron charge-transfer transitions must be to terms in which each of the Fe^{2+} and Fe^{4+} are respectively in spin-quintet terms, 5E or 5T_2 . For each ion on each site we

know the sign and have a good idea of the crystal-field splitting.³⁵ From this we can predict approximately the relative positions of the excited terms. For example, the lowest-energy pair term occurring when an electron has been transferred from the octahedral to the tetrahedral site must have each ion in its respective 5E term. The crystal-field parameter for the Fe^{2+} ion on a tetrahedral oxide site is normally about 4000 cm^{-1} , which is then the energy separation of the 5E and 5T_2 terms of this ion. The second excited-pair term of the pair will, therefore, have the Fe^{2+} in its 5T_2 and the Fe^{4+} in its 5E term and will be higher in energy than the first by approximately 4000 cm^{-1} . Similarly the relative energies of the other excited terms can be derived and are given in Table II.

It is not easy to identify any of these charge-transfer transitions in the spectrum of YIG. It has been suggested⁴³ that the lowest tetrahedral-to-octahedral transition should give a strong diamagnetic line in the MCD spectrum, as is observed at $23\,250\text{ cm}^{-1}$. We have seen, however, that trying to predict the existence of diamagnetic lines is a little unreliable. Instead we think that the best evidence that this transition is a charge-transfer transition is the observation of a conductivity gap of about 2.9 eV both in the photoconductivity⁴⁴ and in thermal-activation experiments.⁴⁵

In the absence of more definitive data the most attractive assignments of the absorption bands of intermediate strength in the region of the spectrum from $20\,000$ to $28\,000\text{ cm}^{-1}$ are to biexciton transitions except for the line at $23\,250\text{ cm}^{-1}$, which is tentatively assigned to a tetrahedral-iron-to-octahedral-iron charge-transfer transition. Even so, it is clear that this region of the spectrum is still not properly understood and more optical and magneto-optical data are needed, particularly that taken from magnetically diluted crystals.

TABLE II. Designation and relative energies of the iron-iron charge-transferred excited terms.

Excited term	Electron transferred from					
	Tetrahedral to octahedral site			Octahedral to tetrahedral site		
	Site	Site	Approximate energy above first excited term (cm^{-1})	Site	Site	Approximate energy above first excited term (cm^{-1})
first	Tet (Fe^{4+}) 5T_2	Oct (Fe^{2+}) ${}^5T_{2g}$	0	Tet (Fe^{2+}) 5E	Oct (Fe^{4+}) 5E	0
second	5T_2	5E_g	10 000	5T_2	5E	4000
third	5E	${}^5T_{2g}$		5E	5T_2	20 000
fourth	5E	5E_g	20 000	5T_2	5T_2	24 000

VI. CONCLUSION

We have used the combination of MCD, FR, and absorption spectra to show that in YIG, all absorption bands but one below $28\,000\text{ cm}^{-1}$ have paramagnetic magneto-optic character. A study of the ${}^6A_{1g}(S) \rightarrow {}^4T_{1g}(G)$ band suggests that its intensity is due to vibronics of magnon sidebands and that Clogston's mechanism for intensity only becomes dominant at very low Fe^{3+} concentrations; this situation is probably the same for all the Fe^{3+} crystal-field bands. However, Clogston's suggestion of spin-orbit mixing of 4T_1 and 6A_1 states is shown to produce a fractional dichroism of the magnitude observed experimentally for the ${}^6A_{1g}(S) \rightarrow {}^4T_{1g}(G)$ band and qualitatively explains the observation of paramagnetic terms in the higher-energy crystal-field transitions. The amount of admixture of 4T_1 states into the ground state to produce the observed fractional dichroism does not create a significant change in the g factor of the ground state.

The origin of the change in sign of the paramagnetic MCD peaks at $25\,200$ and $27\,400\text{ cm}^{-1}$ is not understood and an understanding of the origin of the

line shape of these bands awaits further investigation.

VII. ACKNOWLEDGMENTS

We wish to thank R. F. Pearson for useful discussions and are indebted to J. Hewett for technical assistance and J. M. Robinson for sample polishing. We are also grateful to J. P. van der Ziel for permission to reproduce one of his figures. Some of this work was done while one of us (H. I. R.) was on leave of absence at N. V. Philips Natuurkundig Laboratorium, Eindhoven, and he wishes to thank Dr. R. P. van Staple both for his hospitality and innumerable useful discussions.

Note added in proof. In recent papers Blazey *et al.* [Solid State Commun. **16**, 589 (1975)] and Schirmer *et al.* [Solid State Commun. **16**, 1289 (1975)] have shown very strong evidence for the existence of Fe^{4+} in SrTiO_3 . No EPR signal was seen from the Fe^{4+} so that is still not clear whether it is a real Fe^{4+} ion or an Fe^{3+} ion with a tightly bound hole. A paramagnetic magneto-optic line has been seen by Shen [Phys. Rev. **134**, 661 (1964)] in Eu^{2+} , also an ion with an S ground term.

- ¹J. F. Dillon, J. Phys. Radium **20**, 374 (1959).
²B. Johnson, Brit. J. Appl. Phys. **17**, 1441 (1966).
³G. Zannarchi and P. F. Bongers, J. Appl. Phys. **40**, 1230 (1969).
⁴W. A. Crossley, R. W. Cooper, J. L. Page, and R. P. van Staple, Phys. Rev. **181**, 896 (1969).
⁵P. C. Bailey and A. Goldman, Westinghouse Research Laboratories Report AD No. 240236, 1960 (unpublished).
⁶G. Abulafya and H. Le Gall, Solid State Commun. **11**, 629 (1972).
⁷D. E. Lacklison, G. B. Scott, H. I. Ralph, and J. L. Page, IEEE Trans. Magn. **9**, 457 (1973).
⁸K. Shinagawa, H. Takeuchi, and S. Taniguchi, Jpn. J. Appl. Phys. **12**, 466 (1973).
⁹J. F. Dillon, in *Magnetic Properties of Material*, edited by Jan Smit (McGraw-Hill, New York, 1971).
¹⁰D. Kuse, C. Schüller, and A. Beck, Phys. Status Solidi A **14**, 153 (1972).
¹¹R. Krishnan, H. Le Gall, and Tran Khanh Vien, Phys. Status Solidi A **17**, K65 (1973).
¹²W. Wetzling, B. Andlauer, P. Koidl, J. Schneider, and W. Tolksdorf, Phys. Status Solidi B **59**, 63 (1973).
¹³S. Wittekoek, T. J. A. Popma, and J. M. Robertson, AIP Conf. Proc. **18**, 944 (1973).
¹⁴F. J. Kahn, P. S. Pershan, and J. P. Remeika, Phys. Rev. **186**, 891 (1969).
¹⁵J. C. Canit, J. Badoz, B. Briat, and R. Krishnan, Solid State Commun. **15**, 767 (1974).
¹⁶G. B. Scott, D. E. Lacklison, and J. L. Page, Phys. Rev. B **10**, 971 (1974).
¹⁷J. M. Robertson, M. J. G. van Hout, J. C. Verplanke, and J. C. Brice, Mater. Res. Bull. **9**, 555 (1974).
¹⁸G. B. Scott (unpublished).
¹⁹H. Kato, J. Chem. Phys. **58**, 1964 (1973).
²⁰A. J. McCaffery, P. J. Stephens, and P. N. Schatz, Inorg. Chem. **6**, 1614 (1967).
²¹G. B. Scott, D. E. Lacklison, and J. L. Page, J. Phys. C **8**, 513 (1975).
²²A. M. Clogston, J. Phys. Radium **20**, 151 (1959).
²³P. N. Schatz, R. B. Shiflett, J. A. Spencer, A. J. McCaffery, S. B. Piepho, J. R. Dickinson, and T. E. Lester, Symp. Faraday Soc. **3**, 14 (1969).
²⁴G. A. Osborne, B. D. Bird, P. J. Stephens, J. J. Duffield, and A. Abu-Shumays, Solid State Commun. **9**, 33 (1971).
²⁵J. Ingels and G. Jacobs, Phys. Status Solidi **30**, 163 (1968).
²⁶K. W. Blazey, J. Appl. Phys. **45**, 2273 (1974).
²⁷J. Cheng, Ph.D. thesis (University of Oregon, 1971) (unpublished).
²⁸A. J. McCaffery, Symp. Faraday Soc. **3**, 96 (1969).
²⁹J. P. van der Ziel, J. F. Dillon, and J. P. Remeika, AIP Conf. Proc. **5**, 254 (1971).
³⁰The absorption spectra of YIG and YGdG: Fe have been measured over this whole range and it can be seen that the first transition involving single Fe^{3+} ions occurs at $35\,500\text{ cm}^{-1}$ in YIG. G. B. Scott (unpublished).
³¹J. J. Song, P. B. Klein, R. L. Wadsack, M. Selders, S. Mroczkowski, and R. K. Chang, J. Opt. Soc. Am. **63**, 1135 (1973).
³²D. L. Wood and J. P. Remeika, J. Appl. Phys. **38**, 1038 (1967).
³³S. H. Wemple, S. L. Blank, J. A. Seman, and W. A. Biolsi, Phys. Rev. B **9**, 2134 (1974).
³⁴Y. Tanabe, T. Moyria, and S. Sugano, Phys. Rev. Lett. **15**, 1023 (1965); J. Ferguson, H. J. Guggenheim, and Y. Tanabe, J. Phys. Soc. Jpn. **21**, 692 (1966).
³⁵J. S. Griffith, *The Theory of Transition Metal Ions* (Cambridge U. P., Cambridge, England, 1964).
³⁶K. A. Schroeder, J. Chem. Phys. **37**, 1587 (1962).

- ³⁷J. Ferguson, E. R. Krausz, and H. J. Guggenheim, *Mol. Phys.* 27, 577 (1974).
- ³⁸L. Rimai and T. Kushida, *Phys. Rev.* 143, 160 (1966).
- ³⁹J. Ferguson, *Aust. J. Chem.* 21, 307 (1968); J. Ferguson, H. J. Guggenheim, and Y. Tanabe, *Phys. Rev.* 161, 207 (1967).
- ⁴⁰C. K. Jorgensen, *Mol. Phys.* 4, 235 (1961).
- ⁴¹B. W. Faughnan, *Phys. Rev. B* 4, 3623 (1971).
- ⁴²G. Lehmann, *Z. Phys. Chem. (Neue Folge)* 72, 279 (1970).
- ⁴³S. Wittekoek, T.J.A. Popma, J. M. Robertson, and P. F. Bongers, *Phys. Rev. B* (to be published).
- ⁴⁴P. M. Grant and W. Ruppel, *Solid State Commun.* 5, 543 (1967).
- ⁴⁵R. Metselaar and P. K. Larsen, *Solid State Commun.* 15, 291 (1974).